Published OnlineFirst on November 2, 2010 as 10.1158/1535-7163.MCT-10-0517

The Synthetic Caged *Garcinia* Xanthone Cluvenone Induces Cell Stress and Apoptosis and Has Immune Modulatory Activity

Ayse Batova[1], Diego Altomare[2], Oraphin Chantarasriwong[1], Kari L. Ohlsen[4], Kim E. Creek[3], You-Chin Lin[6], Amy Messersmith[2], Alice L. Yu[5,6], John Yu[7], and Emmanuel A. Theodorakis[1]

Abstract

Several caged *Garcinia* xanthone natural products have potent bioactivity and a documented value in traditional Eastern medicine. Previous synthesis and structure activity relationship studies of these natural products resulted in the identification of the pharmacophore represented by the structure of cluvenone. In the current study, we examined the anticancer activity of cluvenone and conducted gene expression profiling and pathway analyses. Cluvenone was found to induce apoptosis in T-cell acute lymphoblastic leukemia cells (EC_{50} = 0.25 μmol/L) and had potent growth-inhibitory activity against the NCI60 cell panel, including those that are multidrug-resistant, with a GI_{50} range of 0.1 to 2.7 μmol/L. Importantly, cluvenone was approximately 5-fold more potent against a primary B-cell acute lymphoblastic leukemia compared with peripheral blood mononuclear cells from normal donors, suggesting that it has significant tumor selectivity. Comparison of cluvenone's growth-inhibitory profile to those in the National Cancer Institute database revealed that compounds with a similar profile to cluvenone were mechanistically unlike known agents, but were associated with cell stress and survival signaling. Gene expression profiling studies determined that cluvenone induced the activation of mitogen-activated protein kinase and NrF2 stress response pathways. Furthermore, cluvenone was found to induce intracellular reactive oxygen species formation. Lastly, the modulation in the expression of several genes associated with T cell and natural killer cell activation and function by cluvenone suggests a role as an immune-modulator. The current work highlights the potential of cluvenone as a chemotherapeutic agent and provides support for further investigation of these intriguing molecules with regard to mechanism and targets. *Mol Cancer Ther; 9(11); 2869–78. ©2010 AACR.*

Introduction

According to the American Cancer Society, there were nearly 1.5 million men and women diagnosed with cancer in the United States in 2009. It is projected that approximately 40% of these individuals will die of their disease. The current annual cancer incidence rate corresponds to one out of every two men, and one out of every three women being diagnosed with cancer within their lifetime. The main obstacle for successful treatment is resistance to current therapies. Not only are the current chemotherapeutic agents ineffective against many cancers, especially relapsed cancers, but there is significant toxicity associated with these therapies. Therefore, it is essential to intensively investigate novel agents that are not only effective against refractory cancers, but are also tumor selective and thus less toxic.

The tropical trees of the genus *Garcinia*, found in lowland rainforests of Southeast Asia, are widely known for their use in folk medicine (1, 2). Phytochemically, these trees are recognized as a rich source of xanthone and xanthonoid natural products that hold high pharmaceutical potential. Gambogic acid (GA) is the main active component of gamboge, a dry resin secreted from *Garcinia hanburyi*. It has been well established that GA induces apoptosis in multiple tumor cell lines including T47D breast cancer cells and MGC-803 human gastric carcinoma cells at submicromolar to low micromolar concentrations (3–5). Furthermore, GA has shown efficacy in several human tumor xenograft models and has entered clinical trials in China for the treatment of cancer (6–9).

We have previously reported a new strategy for the chemical synthesis of the natural products of *Garcinia* (10, 11). The synthesis is short, efficient, and stereoselective,

Authors' Affiliations: [1]Department of Chemistry and Biochemistry, University of California, San Diego, La Jolla, California; [2]Department of Pathology, Microbiology, and Immunology, University of South Carolina School of Medicine; [3]Department of Pharmaceutical and Biomedical Sciences, South Carolina College of Pharmacy, Columbia, South Carolina; [4]BioData Solutions; [5]Department of Pediatrics, Hematology/Oncology, University of California, San Diego, California; [6]The Genomics Research Center and [7]The Institute of Cellular and Organismic Biology, Academia Sinica, Taipei, Taiwan

Corresponding Author: Ayse Batova, Department of Chemistry and Biochemistry, University of California, 9500 Gilman Drive, La Jolla, CA 92093. Phone: 619-471-9655; Fax: 619-543-5413. E-mail: abatova@ucsd.edu

doi: 10.1158/1535-7163.MCT-10-0517

and allows access to a variety of these compounds and related analogues. This technology not only eliminates the drawbacks of natural supply and varying isomeric mixtures, typical of natural products, but also provides the opportunity to perform systematic biological and pharmacologic studies resulting in the discovery of novel pharmacophores and the development of highly effective chemotherapeutic agents. More recently, we have evaluated the pharmacophoric motif of the caged *Garcinia* xanthones and have identified the minimum bioactive motif of these compounds (12, 13). Based on this information, we have generated a simple synthetic analogue, cluvenone, which was found to induce apoptosis in multidrug-resistant promyelocytic leukemia cells (HL-60/ADR) at nanomolar concentrations, with EC_{50} values equal to that found in the parental cells (HL-60; ref. 13). It is believed that the unique structure of cluvenone and members of the *Garcinia* family of natural products represents a novel pharmacophore that accounts for the cytotoxicity of these compounds against multidrug-resistant cancer cells. In the current study, we describe the anticancer activity and tumor selectivity of cluvenone as well as the results of gene expression profiling and pathway analyses towards the identification of critical molecular determinants in the action of caged *Garcinia* xanthones.

Materials and Methods

Cell lines

T-cell acute lymphoblastic leukemia, CEM, and prostate cancer, PC3, cells were purchased from American Type Culture Collection in 2008. These cell lines were authenticated by observation of morphology and by measuring sensitivity to known agent, GA, and then comparing IC_{50} to that reported in the literature. This testing was done routinely in our laboratory. The NCI60 cell lines screened by the National Cancer Institute (NCI) against cluvenone were not authenticated by the authors.

Apoptosis assay

CEM cells were plated at 10,000 cells/well (96-well plate) in RPMI medium containing 10% fetal bovine serum, 2 mmol/L of glutamine, and 100 units/mL of penicillin/streptomycin (complete medium). Cells were then treated with increasing concentrations of cluvenone or with 0.1% DMSO, and incubated at 37°C for 7 hours before apoptosis was measured using the Cell Death Detection ELISA^{PLUS} kit (Roche Diagnostics GmbH) according to the instructions of the manufacturer. This method constitutes a photometric enzyme immunoassay for the qualitative and quantitative *in vitro* determination of cytoplasmic histone-associated DNA fragments after induced cell death.

Determination of cytotoxicity of cluvenone in the NCI60 cell panel screen

Briefly, cell lines were treated with increasing concentrations of cluvenone for 48 hours and total cell protein was then determined by sulforhodamine B staining. For additional details, please see http://www.dtp.nci.nih.gov/branches/btb/ivclsp.html. The NCI's COMPARE program was used to evaluate the correlation between the growth-inhibitory profile (GI_{50}) of cluvenone and other compounds in the NCI chemical database. In addition, 3D Mind tools (http://spheroid.ncifcrf.gov/spheroid/) was used to determine where cluvenone mapped on a self-organizing map (SOM).

Determination of primary acute lymphoblastic leukemia and peripheral blood mononuclear cell viability

Heparinized bone marrow or peripheral blood samples were obtained at diagnosis or relapse from T-cell acute lymphoblastic leukemia (ALL) patients enrolled in Pediatric Oncology Group Protocols no. 9000 and no. 9400 (ALL Biology Study). In addition, peripheral blood was obtained from normal donors. Mononuclear cells from bone marrow or peripheral blood were isolated by isopyknic sedimentation through Ficoll-Hypaque (specific gravity, 1.077 g/mL; Pharmacia) at 400 × *g* for 30 minutes followed by two washes with RPMI 1640. The content of lymphoblasts in these patient samples, as determined by Wright stain, was ≥80%. Primary B-cell ALL and peripheral blood mononuclear cells (PBMC) obtained from normal donors were treated with increasing concentrations of cluvenone for 48 hours and then viable cell numbers were determined by counting in a hemocytometer.

Agilent Whole Human Genome 4 × 44K arrays

Treatment of cells with cluvenone and isolation of total RNA. CEM cells were treated in quadruplicate with 0.3 μmol/L of cluvenone, or with 0.1% DMSO (control) for 2 and 4.5 hours. Total RNA was isolated from 5×10^6 to 10×10^6 cells using the ArrayGrade Total RNA Isolation Kit (SuperArray Bioscience Corp.) according to the recommendations of the manufacturer. The integrity and concentration of the total RNA was assessed on a 2100 Bioanalyzer (Agilent Technologies), using the RNA 6000 Nano LabChip. The RNA integrity number ranged from 9.5 to 10.0.

Microarray analysis. RNA (500 ng/reaction) was amplified (one round) and labeled with Cyanine 3 (Cy3, control) or Cyanine 5 (Cy5, treated) using the QuickAmp Labeling Kit (Agilent) according to the recommendations of the manufacturer. The labeled amplified RNA was hybridized at 65°C for 17 hours to Agilent Whole Human Genome 4 × 44K microarrays. The arrays were washed with Agilent wash buffers 1 and 2 and then placed in an Agilent Stabilization and Drying Solution according to the directions of the manufacturer. The arrays were scanned on a Perkin-Elmer ProScanArray Express HT scanner. The scanned images were quantified using ImaGene 8.0.1 software from BioDiscovery and significantly differentially expressed genes were identified using GeneSifter from Geospiza. Probes that achieved a significance of $P \leq 0.005$ in the ANOVA analysis with

Benjamini–Hochberg correction were subjected to pathway analysis. The genetic loci corresponding to each probe, together with the fold change at both the 2- and the 4.5-hour time points, were analyzed using Ingenuity Pathway Analysis software (Ingenuity Systems, Inc.) and the Pathway-Express Tool, created by Sorin Draghici at Wayne State University (available at http://vortex.cs.wayne.edu/ontoexpress), to assess affected pathways.

Unlike other pathway analysis methods, The Pathway-Express Tool conducts an impact analysis that includes the classical statistics, but also considers other crucial factors such as the magnitude of each gene's expression change, their type and position in the given pathways, and their interconnectedness, thus representing a systems biology approach (14). The impact factor is equivalent to the negative log of the global probability of having both a statistically significant number of differentially expressed genes, and a large perturbation in the given pathway. Thus, impact factor values indicate the likelihood that the listed pathway is truly affected in the treated case, and is not a spurious result.

Real-time reverse transcription-PCR

cDNA was transcribed using the iScript cDNA Synthesis Kit (Bio-Rad). All cDNA reaction mixtures included 50 ng of template RNA. The reverse transcriptase PCR reactions were done on an Applied Biosystems GeneAmp PCR System 2700 using the temperature cycling conditions recommended in the iScript cDNA Synthesis Kit protocol. The temperature cycling conditions included 5 minutes at 25°C, 30 minutes at 42°C, and 5 minutes at 85°C. Real-time PCR reactions were done on each cDNA sample to quantify the selected genes. Primer sequences for HSPA1A (forward, 5′-GCCGAGAAGGACGAGTTTGA-3′; reverse, 5′-TCCGCTGATGATGGGGTTAC-3′) were determined using RTPrimerDB (http://www.rtprimerdb.org/). Actin (forward, 5′-CGTGGACATCCGCAAAGAC-3′; reverse, 5′-AGGGTGTAACGCAACTAAG-3′) was used as a control for each cDNA sample. Primers were purchased from Integrative DNA Technologies. The primers were combined in equal volumes to create a primer mix with a final concentration of 5 μmol/L per primer. Each 25 μL PCR reaction included 5 μL of water, 12.5 μL of iQ Sybr Green Supermix (Bio-Rad), 5 μL of 5 μmol/L primer mix, and 2.5 μL of cDNA sample. Real-time PCR reactions were done on a MyiQ Single-Color Real-time PCR Detection System (Bio-Rad). The thermal cycler protocol consisted of an initial denaturation at 95°C for 30 seconds, followed by 50 cycles of 95°C denaturation for 10 seconds, annealing for 50 seconds at gene-specific temperature, and by an extension at 60°C for 1 minute. The final step of the protocol included a melt curve from 60°C to 100°C in 0.5°C interval at 10 seconds per interval.

Measurement of intracellular reactive oxygen species

The human prostate cancer cell line PC3 was plated in a 96-well plate at 5×10^4 cells/well in complete RPMI and incubated overnight. The cells were treated with up to 1 μmol/L of cluvenone or with 0.1% DMSO (control) for 1, 2, 5.5, or 15 hours. In addition, cells were treated with increasing concentrations of H_2O_2 as a control for reactive oxygen species (ROS) induction. To measure ROS, cells were loaded with 0.2 mmol/L of DCFH-DA for 45 minutes at 37°C using the OxiSelect ROS Assay kit (Cell Biolabs, Inc.) according to the recommendations of the manufacturer. Fluorescence was measured on a Synergy Mx plate reader (BioTek Instruments, Inc.) with excitation/emission at 480/530 nmol/L.

Measurement of cluvenone cytotoxicity in the presence of *N*-acetylcysteine

PC3 cells were plated in a 96-well plate at 1×10^4 cells/well in complete RPMI and incubated overnight. The following day, cells were treated for 48 hours with 0.1% DMSO or 1 μmol/L of cluvenone in the presence or absence of *N*-acetylcysteine at 0.1, 1, and 5 mmol/L. Cells were pulsed for 6 hours with ^{3}H-thymidine and incorporation was measured in a scintillation counter (Beckman Coulter, Inc.) after cells were washed and deposited onto glass microfiber filters using a cell harvester M-24 (Brandel).

Results

In a previous report (12), we screened a number of different caged *Garcinia* xanthones against solid and nonsolid tumor cell lines including multidrug-resistant HL-60 cells (HL-60/ADR) expressing P-glycoprotein (15). We found that cluvenone (Fig. 1, inset) was the most potent of the synthetic analogues with equal or similar activity to the structurally more complex parent natural product, GA. More importantly, cluvenone, like GA, was equally toxic to HL-60/ADR as the parental

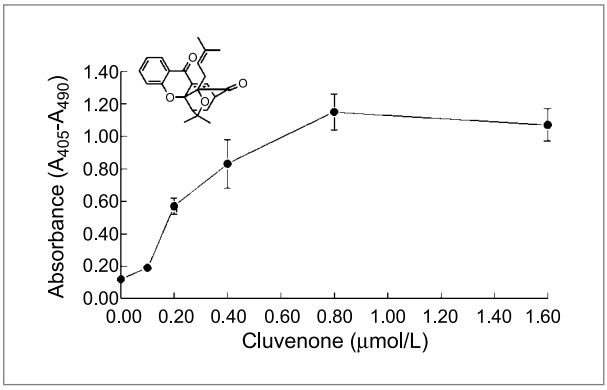

Figure 1. Structure of cluvenone (inset) and induction of apoptosis by cluvenone in CEM cells. CEM cells were plated into a 96-well plate at 10,000 cells/well and were treated with 0.1% DMSO or cluvenone at increasing concentrations. After incubation at 37°C for 7 h, apoptosis was measured using the Cell Death Detection ELISA^{PLUS} kit. All conditions were conducted in triplicate. Points, mean; bars, SD.

HL-60 cell line. The mechanism of cytotoxicity of cluvenone was examined in leukemia cell lines using a cell death detection ELISA assay which measures histone-associated DNA fragments. Cluvenone induced apoptosis in a dose-dependent manner in the T cell ALL cell line, CEM, characterized by having mutated *p53* and deletion of *p15* and *p16*, genes frequently inactivated in multiple cancers (Fig. 1). The EC_{50} of

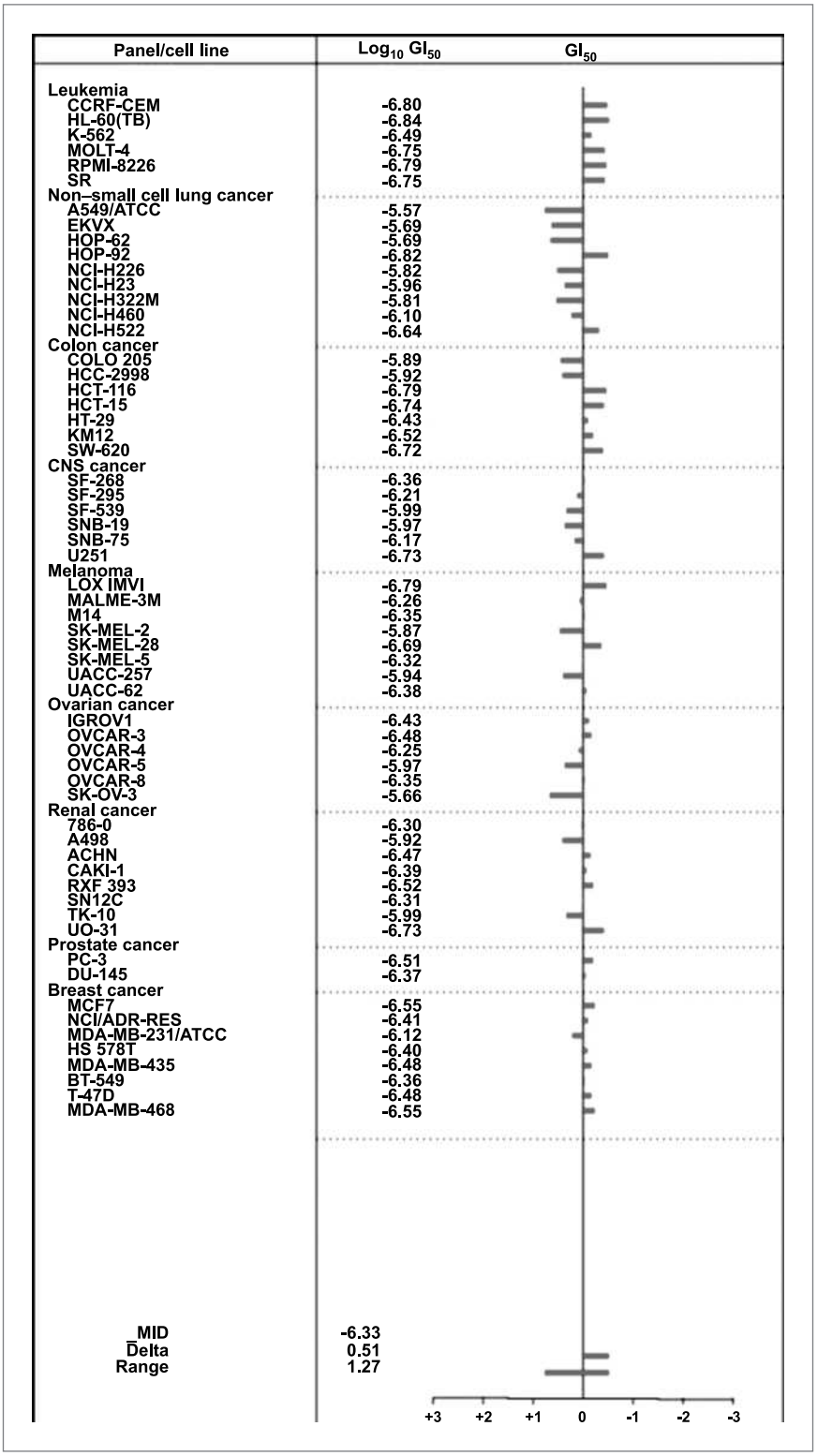

Figure 2. Cluvenone induces potent inhibition of proliferation in multiple solid and nonsolid tumor cells. NCI60 cell lines were treated with increasing concentrations of cluvenone for 48 h and total cell protein was then determined by sulforhodamine B staining and GI_{50} was determined.

cluvenone in CEM was 0.25 μmol/L after 7.5 hours of treatment and the characteristic morphology of apoptotic death, membrane blebbing, was visible as early as within 4 hours of treatment (data not shown). Similar results were obtained using HL-60 and HL-60/ADR cells with an EC_{50} of 0.25 and 0.32 μmol/L, respectively (13), indicating that the cytotoxicity of cluvenone is not affected by the expression of P-glycoprotein or by the absence of *p53* and cell cycle inhibitory genes.

Encouraged by these results, cluvenone was then screened against the NCI60 cell panel to extend the evaluation of its cytotoxicity and, more importantly, gain insight into its possible mode of action. The results of the NCI60 cell panel screen confirmed that cluvenone is cytotoxic to all cancer cell lines tested including those that are multidrug-resistant, with a mean GI_{50} of 0.5 μmol/L (range, 0.1–2.7 μmol/L; Fig. 2). For example, even a robustly multidrug-resistant cell line such as NCI/ADR-RES (breast) as well as others such as HCT15 (colon) and U031 (renal) were sensitive to cluvenone with a GI_{50} of <0.5 μmol/L, with the exception of TK10 (renal) which had a GI_{50} of 1.0 μmol/L (Fig. 2). Additionally, tumor cells with very aggressive growth and metastatic potential such as NCIH460 (large cell lung cancer) and LOX (melanoma) were also sensitive to cluvenone with a GI_{50} of 786 and 163 nmol/L, respectively. Collectively, these results suggest that cluvenone and members of this class of *Garcinia* xanthones might overcome the drug resistance typical of relapsed cancers.

Although cluvenone is cytotoxic to a broad range of tumor cells including multidrug-resistant cancer cells, it must show tumor selectivity to be an effective chemotherapeutic agent. To determine whether cluvenone has any selectivity for cancer cells over normal cells, we examined the effect of cluvenone in a primary human leukemia and PBMC obtained from a normal donor. Previously, we have found that cytotoxicity results from viability assays using primary cells from normal donors and patients correlates well with *in vivo* data, as opposed to data from similar assays using cell lines (15). For these experiments, primary cells were exposed to increasing concentrations of cluvenone for 48 hours and then viable cell numbers were determined. The results shown in Fig. 3 indicate that cluvenone is 4.7-fold more toxic to leukemia cells (IC_{50} = 1.1 μmol/L) than PBMC from normal donors (IC_{50} = 5.2 μmol/L). Interestingly, in the same experiment, GA was 3.9-fold more toxic to B-ALL cells than PBMC, suggesting that it may have greater toxicity to normal cells compared with cluvenone (data not shown). The observed differential cytotoxicity of cluvenone against leukemia cells versus PBMC from normal individuals is extremely encouraging as standard chemotherapeutic agents are generally similarly toxic to PBMC and tumor cells. Based on the observed tumor selectivity, it is anticipated that cluvenone will be well-tolerated at the low doses which are therapeutically effective.

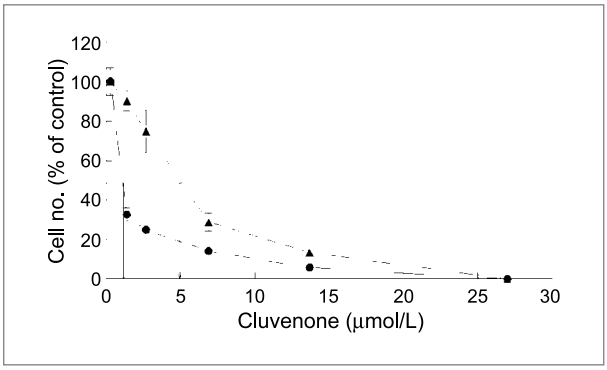

Figure 3. Cluvenone has selective toxicity against leukemia cells compared with PBMC from normal donors. Primary B-ALL cells and PBMC obtained from a normal donor were treated with increasing concentrations of cluvenone for 48 h and then viable cell numbers were determined by counting in a hemocytometer. All conditions were conducted in triplicate. Points, mean; bars, SD (●, B-ALL; ▲, PBMC).

To gain insight into the mechanism of action of cluvenone, a COMPARE analysis was conducted using the results of the NCI60 cell panel screen. The results of this analysis determined that molecules with a similar cytotoxicity profile to cluvenone were of completely different chemical structures (Fig. 4A), and were not similar to standard agents. Furthermore, using 3D Mind tools, the top six ranked molecules and GA were mapped to the Q region of a SOM, distal to agents with known mechanisms of action (Fig. 4B). The Q region of the SOM includes bioactive molecules with yet unknown mechanisms of action but which have recently been implicated to activate signaling pathways involved in cell stress and survival (16, 17). These findings highlight the structural uniqueness of cluvenone and members of the caged *Garcinia* xanthones as well as showing the potential of the current research for therapeutic application to cancers refractory to standard chemotherapy.

Intrigued by the results of the SOM suggesting a novel mechanism of action, and to further investigate the mode of action of cluvenone, gene expression profiling experiments were conducted using Agilent Whole Genome 4 × 44K arrays (accession no. GSE23536 in the GEO database). In these experiments, CEM cells were treated in quadruplicate with vehicle (DMSO) or with 0.3 μmol/L of cluvenone for 2 and 4.5 hours. Analysis of the microarray data using GeneSifter software revealed that 191 or 250 genes were altered in expression at least 1.7-fold (adjusted $P < 0.005$) by cluvenone treatment for 2 or 4.5 hours, respectively. The fold change cutoff was selected based on a report of an independent laboratory demonstrating decreased expression of telomerase reverse transcriptase in response to treatment with GA (18, 19). In agreement with this report, our data indicated that telomerase reverse transcriptase expression was decreased 1.7-fold by cluvenone indicating that a 1.7-fold change in expression was a valid cutoff.

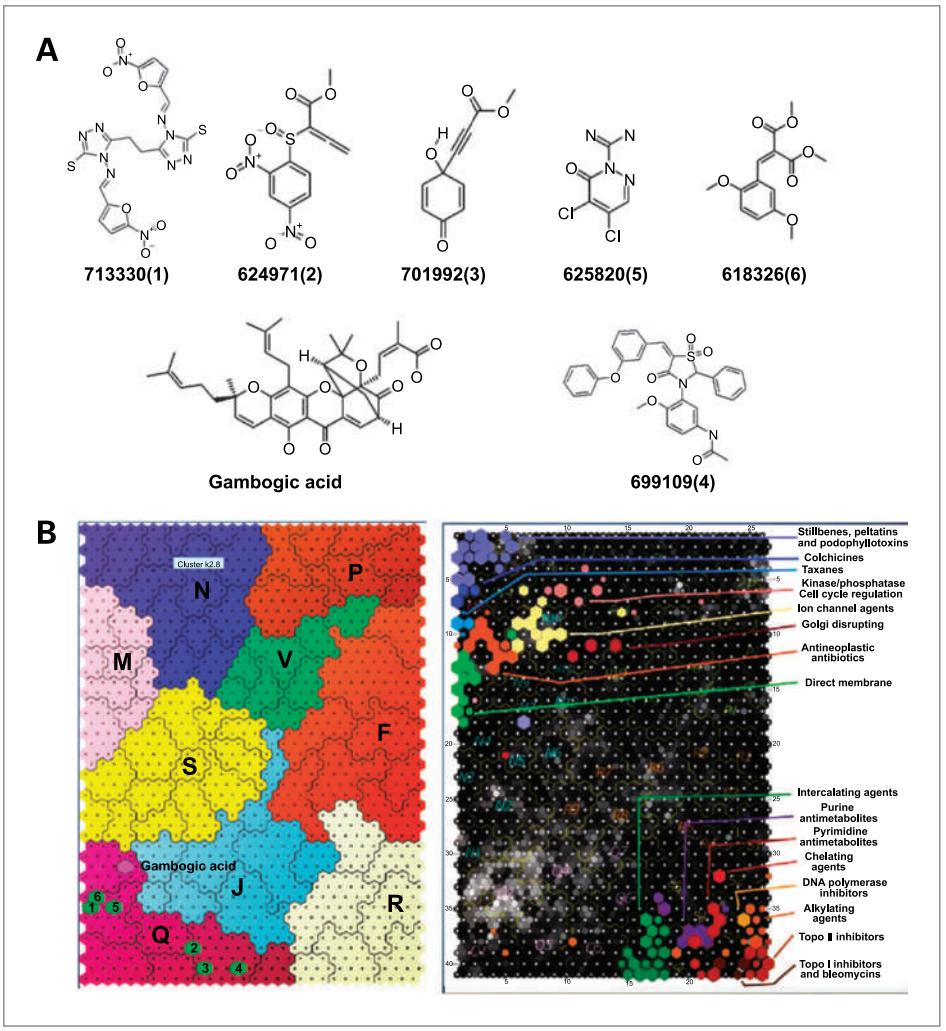

Figure 4. GA and the top six ranked compounds in NCI database with similar antiproliferation activity profile to cluvenone map to the Q region of a SOM. The NCI's COMPARE program was used to evaluate the correlation between the cytotoxicity profile (GI_{50}) of cluvenone and other compounds in the NCI chemical database. In addition, 3D Mind tools (http://spheroid.ncifcrf.gov/spheroid/) was used to determine where the top-ranked compounds mapped on a SOM. A, structures of the top six ranked compounds with NCI database identifier number followed by numbers in parentheses corresponding to positions on the SOM. B, SOM with the positions of top-ranked compounds relative to those of known agents.

The list of significantly altered genes at both times (2 and 4.5 h) of cluvenone treatment were analyzed using Pathway-Express software to determine which cell signaling pathways would be affected. The results, summarized in Table 1, reveal that one of the most significantly affected pathways, at both time points of the treatment, includes the mitogen-activated protein kinase (MAPK) cell stress signaling pathway as evidenced by the dramatic and progressive upregulation of the heat shock gene, *HSPA1A*, in addition to upregulation of *HSPA8* and *MAPK14*, also known as p38. The dramatic upregulation of *HSPA1A* mRNA by cluvenone treatment for 2 and 4.5 hours, as determined by microarray analysis, was confirmed by real-time reverse transcription-PCR (data not shown). Analysis of the gene expression data using Ingenuity Pathway Analysis software confirmed oxidative cell stress signaling to be a predominant pathway activated in response to cluvenone. In particular, Nrf2-mediated oxidative stress signaling which is downstream of MAPK signaling, and a defense mechanism against oxidative stress (20), seemed to be activated ($P = 9.09 \times 10^{-4}$). This result was based on changes in the expression (≥1.9-fold) of the following stress-associated genes: *DNAJA1, DNAJA4, DNAJA6, DNAJB1, DNAJB2, FTL, FTH1*, and *FKBP5*.

HSPA1A and other heat shock proteins, known to be associated with cell stress, are also involved in antigen processing and presentation (21), as well as in apoptotic signaling in prostate cancer (22) and possibly other cancer cells. Prostate cancer cells, especially at the advanced stages of prostate cancer, are constitutively under oxidative stress resulting in the induction of heat shock proteins which block apoptosis (23). In such cells, the additional oxidative stress imposed by cluvenone, would be expected to result in apoptosis. It is well established that when cell stress is too high for protective mechanisms to overcome damage, cells undergo apoptosis. The induction of *MAPK14*, *Jun*, and *caspase 9* by cluvenone is consistent with the induction of apoptosis via the MAPK-dependent pathway (24). In summary, the induced expression of heat shock genes by cluvenone could affect antigen processing and

presentation in antigen-presenting cells, as well as apoptosis in cancer cells.

Treatment of CEM cells with cluvenone seems to significantly affect adherens junction signaling (Table 1A). Although this result is based on a small change (−1.7-fold) in the T cell–specific transcription factor (*TCF7*), this gene is central in adherens junction signaling involving the Wnt pathway. Furthermore, deregulated transcription of the full-length *TCF7* isoform seems to be involved in prostate and colon cancers (25–27). This may be due, in part, to the transcriptional activation of c-myc by complexes of β-catenin and members of the TCF family ultimately resulting in enhanced cell proliferation (28). Interestingly, cluvenone decreased the expression of both *TCF7* and c-*myc* (>2-fold) suggesting that it may have a role in suppressing signaling through the Wnt pathway associated with prostate and colon cancer (29).

Genes that are central to the regulation of the actin cytoskeleton, *ITGAV* and *ITGB2*, are significantly upregulated by cluvenone at both time points (Table 1A and B), suggesting that cluvenone could affect activities associated with the actin cytoskeleton such as cell motility and adhesion. These activities are particularly important for T-cell function as is protein export (Table 1B), also found to be modulated by cluvenone. Further evidence suggesting regulation of T-cell function by cluvenone is the induction in the expression of *CD69* (2.7-fold), an early leukocyte activation molecule expressed transiently in activated immune cells including T cells (30). Other genes involved in immune function that were found to be upregulated (~2-fold) by cluvenone include *IL11RA* and IL2-inducible T-cell kinase, *ITK*.

Collectively, analyses of the gene expression array results indicate that cluvenone induces Nrf2-mediated oxidative stress and activation of the MAPK-dependent apoptotic pathway. Furthermore, cluvenone seems to have a role in modulating immune function and in regulating adherens junction signaling.

To determine whether cell stress induced by cluvenone is due to the formation of ROS, the levels of ROS were measured in PC3 (prostate cancer) cells treated with cluvenone for various times up to 15 hours using a fluorescence-based assay. The results shown in Fig. 5A, indicate that cluvenone induced ROS formation in a dose-dependent manner within 5.5 hours. Although the level induced was only 30% above control at the highest concentration of cluvenone tested, this level was equivalent to that induced by 1 mmol/L of H_2O_2 and was sufficient to induce apoptosis. As PC3 cells are under constitutive oxidative stress, the increase of ROS levels to 30% above control seems to surpass the capability of protective mechanisms to prevent apoptosis. Induction of ROS by cluvenone was also time-dependent as ROS was not detectable at times tested earlier than 5.5 hours (data not shown). To determine whether induction of ROS accounted for the cytotoxicity of cluvenone, PC3 cells were treated with cluvenone in the presence and absence of the antioxidant,

Table 1. Cell signaling pathways modulated by cluvenone

Pathway	Impact factor	*P*	Genes (fold change)
(A)			
Adherens junction	21.8	8.040×10^{-9}	*TCF7* (–1.7)
MAPK	20.5	2.766×10^{-8}	*HSPA1A* (26.9), *MAPK14* (1.7)
Antigen processing and presentation	9.6	6.968×10^{-4}	*HSPA1A* (26.9), *HSP90AA1* (2.6), *HSP90AB1* (2.2)
Regulation of actin cytoskeleton	7.1	6.867×10^{-3}	*ITGB2* (1.8), *ITGAV* (2.4)
Prostate cancer	6.5	1.065×10^{-2}	*TCF7* (–1.7), *HSP90AB1* (2.2), *HSP90AA1* (2.6), *CASP9* (1.7)
Pathways in cancer	5.6	2.292×10^{-2}	*MSH2* (–1.7), *CASP9* (1.7), *HSP90AB1* (2.2), *TCF7* (–1.7), *ITGAV* (2.4), *CEBPA* (–1.8), *HSP90AA1* (2.6)
(B)			
MAPK	23.8	1.197×10^{-9}	*HSPA1A* (45.1), *HSPA8* (2.9), *CASP3* (–1.8)
Antigen processing and presentation	11.5	1.214×10^{-4}	*HSP90AB1* (2.0), *HSPA1A* (45.1), *HSP90AA1* (3.4), *HSPA8* (2.9)
Regulation of actin cytoskeleton	8.3	2.376×10^{-3}	*ITGAV* (2.8)
Protein export	6.0	1.716×10^{-2}	*OXA1L* (2.3), *SRP9* (1.8)

NOTE: Probes that achieved a significance of $P \leq 0.005$ in ANOVA with Benjamini–Hochberg correction were subjected to pathway analysis using the Pathway-Express Tool created by Sorin Draghici at Wayne State University and available at http://vortex.cs.wayne.edu/ontoexpress. The genetic loci corresponding to each probe together with the fold change at both the 2 h (A) and the 4.5 h (B) time points were analyzed to assess the affected pathways.

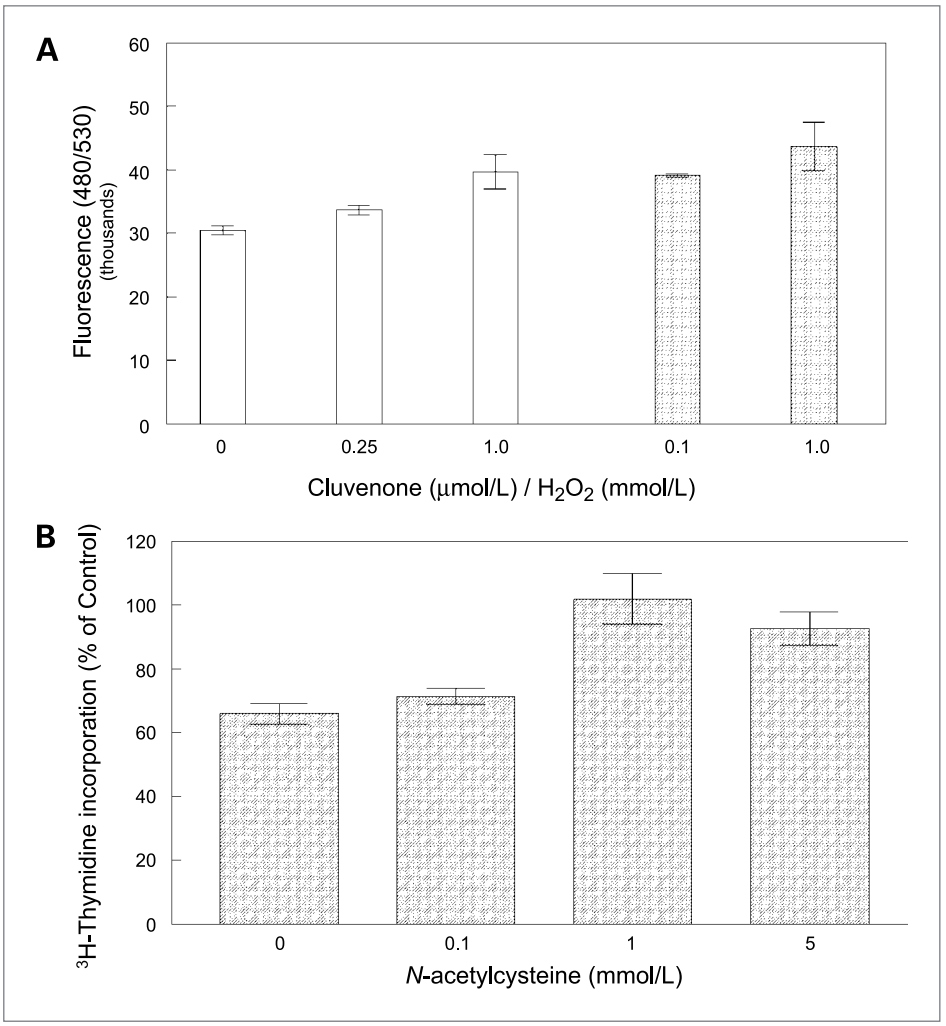

Figure 5. Cluvenone induces cell stress via ROS formation in PC3 cells. A, levels of intracellular ROS were measured by a fluorescence assay in cells treated with up to 1 μmol/L of cluvenone or with 0.1% DMSO (control) for 5.5 h. In addition, cells were treated with increasing concentrations of H_2O_2 as a control for ROS induction. Fluorescence was measured with excitation/emission at 480/530 nmol/L. Clear columns, cluvenone; hatched columns, H_2O_2. B, cytotoxicity of cluvenone (1 μmol/L) in PC3 cells was measured in the presence of increasing concentrations of *N*-acetylcysteine after a 48-h incubation in a ^{3}H-thymidine incorporation assay.

N-acetylcysteine. Cell proliferation was then measured after 48 hours in a ^{3}H-thymidine incorporation assay. The results shown in Fig. 5B showed that *N*-acetylcysteine was able to reduce the cytotoxicity of cluvenone with complete inhibition of cluvenone cytotoxicity at 1 mmol/L of *N*-acetylcysteine. Collectively, these results suggest that the induction of ROS is responsible for the induction of cell stress and apoptosis by cluvenone in PC3 cells. How cluvenone induces ROS and whether additional mechanisms account for cluvenone's cytotoxicity in other cell types remains to be determined.

Discussion

The simple synthetic GA analogue, cluvenone, has significant cytotoxicity at nanomolar concentrations against a broad range of tumor types including multidrug-resistant tumors with leukemia being the most sensitive tumor type, followed by colon, breast, prostate, and renal cancers. Because breast, prostate, and colon cancers are among the most common cancers in the United States, cluvenone may have significant value as a chemotherapeutic agent. Our results indicate that cluvenone is an effective inducer of apoptosis, a required attribute for an effective chemotherapeutic agent. Furthermore, the observed differential cytotoxicity between leukemia cells and PBMC from normal donors, suggesting that cluvenone has tumor selectivity, further adds to the potential value of cluvenone in the treatment of cancer.

The unique structure and activity profile of cluvenone is consistent with the results of the COMPARE analysis indicating that compounds most similar to cluvenone map to the Q region of a SOM, a region including molecules with unknown mechanisms of action, but associated with signaling involved in cell stress and survival. Cellular stress generated by cluvenone seems to be due to the generation of ROS as determined for GA (31). In a recent study, GA induced the formation of ROS in hepatoma cells resulting in loss of mitochondrial membrane potential, release of cytochrome *c*, and apoptosis.

Furthermore, these activities were associated with phosphorylation of JNK and p38, key members of the MAPK stress signaling pathway. Interestingly, the antioxidant, *N*-acetylcysteine, only partly reversed the activation of JNK and p38, and the induction of apoptosis in GA-treated cells, suggesting that additional mechanisms account for the cytotoxicity of GA. Like many natural products, both GA and cluvenone likely have multiple targets and mechanisms of action. For instance, in addition to inducing ROS, GA has been shown to bind to and inhibit the anti-apoptotic activities of the Bcl-2 family of proteins (32). These activities would result in a two-pronged attack on tumor cells with the induction of cell stress and the release of an apoptotic block, not uncommon in tumor cells.

Most recently, it has been reported that the oxidative stress induced by GA results in DNA damage as detected by a comet assay and evidenced by the activation of p53/p21 through the ATR-Chk1 pathway (33). It is important to note, however, that activation of DNA damage response pathways can occur in the absence of DNA strand breaks, in response to alteration in chromatin structure, or to depletion of nucleotide pools (34). Furthermore, it is important to appreciate that DNA damage measured in the comet assay is not necessarily a result of direct genotoxicity as mitochondrial or membrane damage could cause extensive DNA fragmentation via apoptosis or necrosis (35). Whether cluvenone induces DNA damage is yet to be determined. However, the results of the Agilent Whole Genome array analysis did not indicate increased expression, at either time point, of genes encoding DNA repair enzymes including but not limited to RAD17, RAD51, PARP1,2, POL B, or POLG typically induced upon DNA damage (36). Furthermore, neither cluvenone nor GA map to a region to which known DNA damage–inducing agents map on a SOM.

The mitochondria have recently emerged as an important target for cancer therapy due to the bioenergetic differences between normal and cancer cell mitochondria (37). In addition, the mitochondria are an invariant target common to all cells and in which mutations are very rare (37). The rare mutation event in mitochondria suggests a low probability for the development of resistance to agents targeting mitochondria. It is well-established that many mitocans target components of the electron redox chain, leading to ROS production and activation of the intrinsic pathway of apoptosis in cancer cells. Examples of such drugs include the vitamin E analogue, α-TOS, and *N*-(4-hydroxyphenyl) retinamide (4-HPR, fenretinide). The pro-oxidant mechanism of 4-HPR activity has not been clearly identified, although it is likely to act as an inhibitor of at least one of the complexes along the electron transport chain (38). We anticipate cluvenone to be a member of this class of mitocans because it seems to induce oxidative stress resulting in increased expression of caspase 9 (characteristic of intrinsic apoptosis pathway) and apoptosis. Furthermore, the slow induction of ROS by cluvenone, suggesting the presence of certain events prior to the formation of ROS, is consistent with the release of ROS as a consequence of disruption of the mitochondria. Future work is aimed at investigating this possibility.

In addition to the induction of oxidative cell stress, the results of our gene expression array data indicate the induction of several genes associated with T-cell activation and function, as well as natural killer cell function. These genes include those encoding adhesion molecules expressed in resting and activated T cells (integrin-α5 and integrin-β2) as well as a differentiation marker (CD69), and ITK, a kinase involved in regulating natural killer cell–mediated cytotoxicity (39). These results suggest that cluvenone may have significant immunoregulatory functions that may contribute to its anticancer activity. Previous reports on the effects of GA on immune function support our findings. For instance, in one study, GA was found to activate T lymphocytes to induce cancer cell apoptosis in H22 transplanted mice thereby inhibiting tumor growth and extending survival (40).

Clearly, cluvenone, like GA and other natural products, has multiple actions including induction of cellular stress and apoptosis, modulation of immune function, possibly resulting in T cell and natural killer cell–mediated anticancer responses. It is likely that additional mechanisms exist that contribute to the anticancer effects of cluvenone as several genes with unknown function are modulated by cluvenone. Hence, cluvenone seems to be a multitarget anticancer agent with apparent tumor selectivity and the ability to circumvent known mechanisms of chemoresistance. These findings show the clinical potential of cluvenone as a chemotherapeutic agent and support further preclinical investigation. Importantly, however, the identification of multiple targets of cluvenone will be critical to its development as a chemotherapeutic agent and may also lead to the discovery of even more effective anticancer agents.

Disclosure of Potential Conflicts of Interest

No potential conflicts of interest were disclosed.

Acknowledgments

We gratefully acknowledge The Developmental Therapeutics Program of the NCI for conducting screening of cluvenone against the NCI60 cell panel. In addition, we thank Dr. James Zapf for his assistance in generating the SOM with positions of molecules having similar mechanism(s) of action to cluvenone.

Grant Support

NIH grant CA 133002 (E. Theodorakis) and, in part, by funds from Academia Sinica (A.L. Yu). The gene expression profiling studies were conducted at the University of South Carolina DNA Microarray Facility, supported in part by NIH grant number P20 RR-016461 from the National Center for Research Resources.

The costs of publication of this article were defrayed in part by the payment of page charges. This article must therefore be hereby marked *advertisement* in accordance with 18 U.S.C. Section 1734 solely to indicate this fact.

Received 06/08/2010; revised 09/09/2010; accepted 09/15/2010; published OnlineFirst 11/02/2010.

References

1. Ollis WD, Redman BT, Sutherland IO, Jewers K. The constitution of bronianone. J Chem Soc Chem Commun 1969:879–80.
2. Kumar P, Baslas RK. Phytochemical and biological studies of the plants of the genus Garcinia. Herb Hung 1980;19:81–91.
3. Asano J, Chiba K, Tada M, Yoshii T. Cytotoxic xanthones from *Garcinia hanburyi*. Phytochemistry 1996;41:815–20.
4. Zhang H-Z, Kasibhatla S, Wang Y, et al. Discovery, characterization and SAR of gambogic acid as a potent apoptosis inducer by a HTS assay. Bioorg Med Chem 2004;12:309–17.
5. Zhao L, Guo Q-L, You Q-D, Wu Z-Q, Gu H-Y. Gambogic acid induces apoptosis and regulates expressions of Bax and Bcl-2 protein in human gastric carcinoma MGC-803 cells. Biol Pharm Bull 2004;27:998–1003.
6. Yang Y, Yang L, You QD, et al. Differential apoptotic induction of gambogic acid, a novel anticancer natural product, on hepatoma cells and normal hepatocytes. Cancer Lett 2007;256:259–66.
7. Guo QL, You QD, Wu ZQ, Yuan ST, Zhao L. General gambogic acids inhibited growth of human hepatoma SMMC-7721 cells *in vitro* and in nude mice. Acta Pharmacol Sin 2004;25:769–74.
8. Qiang L, Yang Y, You Q-D, et al. Inhibition of glioblastoma growth and angiogenesis by gambogic acid: an *in vitro* and *in vivo* study. Biochem Pharmacol 2008;75:1083–92.
9. Zhou ZT, Wang JW. Phase I human tolerability trial of gambogic acid. Chin J New Drugs 2007;16:79–83.
10. Tisdale EJ, Vong BG, Li H, Kim SH, Chowdhury C, Theodorakis EA. Total synthesis of Secolateriflorone. Tetrahedron 2003;59:6873–87.
11. Tisdale EJ, Slobodov I, Theodorakis EA. Unified synthesis of caged Garcinia natural products based on a site-selective Claisen/Diels-Alder/Claisen rearrangement. Proc Nat Acad Sci U S A 2004;101:12030–5.
12. Batova A, Lam T, Wascholowski V, Yu A, Giannis A, Theodorakis EA. Synthesis and evaluation of caged Garcinia xanthones. Org Biomol Chem 2007;5:494–500.
13. Chantarasriwong O, Cho WC, Batova A, et al. Evaluation of the pharmacophoric motif of the caged Garcinia xanthones. Org Biomol Chem 2009;7:4886–94.
14. Draghici S, Khatri P, Tarca AL, et al. A systems biology approach for pathway level analysis. Genome Res 2007;17:1537–45.
15. Batova A, Shao LE, Diccianni MB, et al. The histone deacetylase inhibitor AN-9 has selective toxicity to acute leukemia and drug-resistant primary leukemia and cancer cell lines. Blood 2002;100:3319–24.
16. Rabow AA, Shoemaker RH, Sausville EA, Covell DG. Mining the National Cancer Institute's tumor-screening database: identification of compounds with similar cellular activities. J Med Chem 2002;45:818–40.
17. Covelle DG, Wallquist A, Huang R, Thanki N, Rabow AA, Lu X-J. Linking tumor cell cytotoxicity to mechanism of drug action: an integrated analysis of gene expression, small-molecule screening and structural databases. Proteins 2005;59:403–33.
18. Wu ZQ, Guo Q-L, You Q-D, Zhao L, Gu H-Y. Gambogic acid inhibits proliferation of human lung carcinoma SPC-A1 cells *in vivo* and *in vitro* and represses telomerase activity and telomerase reverse transcriptase mRNA expression in the cells. Biol Pharm Bull 2004;27:1769–74.
19. Yu J, Guo Q-L, You Q-D, et al. Repression of telomerase reverse transcriptase mRNA and hTERT promoter by gambogic acid in human gastric carcinoma cells. Cancer Chemother Pharmacol 2006;58:434–43.
20. Owuor ED, Kong AN. Antioxidants and oxidants regulated signal transduction pathways. Biochem Pharmacol 2002;64:765–70.
21. Javid B, MacAry PA, Lehner PJ. Structure and function: heat shock proteins and adaptive immunity. J Immunol 2007;179:2035–40.
22. Byun J, Logothetis CJ, Gorlov IP. Housekeeping genes in prostate tumorigenesis. Int J Cancer 2009;125:2603–8.
23. Kirshner JR, He S, Balasubramanyam V, Kepros J, Yang CY, Zhang M. Elesclomol induces cancer cell apoptosis through oxidative stress. Mol Cancer Ther 2008;7:2319–27.
24. Sumbayev VV, Yasinska IM. Role of MAP kinase-dependent apoptotic pathway in innate immune responses and viral infection. Scand J Immunol 2006;63:391–400.
25. Waterman M. Expression of lymphoid enhancer factor/T-cell factor proteins in colon cancer. Curr Opin Gastroenterol 2002;18:53–9.
26. Cronauer MV, Schulz WA, Ackermann R, Burchardt M. Effects of WNT/β-catenin pathway activation on signaling through T-cell factor and androgen receptor in prostate cancer cell lines. Int J Oncol 2005;26:1033–40.
27. Waterman M. Lymphoid enhancer factor/T cell factor expression in colorectal cancer. Cancer Metastasis Rev 2004;23:41–52.
28. He TC, Sparks AB, Rago C, et al. Identification of c-myc as a target of the APC pathway. Science 1998;281:1509–12.
29. Chen S, Guttridge DC, You Z, et al. Wnt-1 signaling inhibits apoptosis by activating β-catenin/T cell factor-mediated transcription. J Cell Biol 2001;152:87–96.
30. Sancho D, Gómez M, Sánchez-Madrid F. CD69 is an immunoregulatory molecule induced following activation. Trends Immunol 2005;26:136–40.
31. Nie F, Zhang X, Qi Q, et al. Reactive oxygen species accumulation contributes to gambogic acid-induced apoptosis in human hepatoma SMMC-7721 cells. Toxicology 2009;260:60–7.
32. Zhai D, Jin C, Shiau CW, Kitada S, Satterthwait AC, Reed JC. Gambogic acid is an antagonist of antiapoptotic Bcl-2 family proteins. Mol Cancer Ther 2008;7:1639–46.
33. Rong JJ, Hu R, Song XM, et al. Gambogic acid triggers DNA damage signaling that induces p53/p21(Waf1/CIP1) activation through the ATR-Chk1 pathway. Cancer Lett 2010;296:55–64.
34. Bakkenist CJ, Kastan MB. DNA damage activates ATM through intermolecular autophosphorylation and dimer dissociation. Nature 2003;421:499–506.
35. Olive PL, Banáth JP. The comet assay: a method to measure DNA damage in individual cells. Nat Protoc 2006;1:23–9.
36. Lieberman HB. DNA damage repair and response proteins as targets for cancer therapy. Curr Med Chem 2008;15:360–7.
37. Ralph SJ, Rodríguez-Enríquez S, Neuzil J, Moreno-Sánchez R. Bioenergetic pathways in tumor mitochondria as targets for cancer therapy and the importance of the ROS-induced apoptotic trigger. Mol Aspects Med 2010;31:29–59.
38. Ralph SJ, Neuzil J. Mitochondria as targets for cancer therapy. Mol Nutr Food Res 2009;53:9–28.
39. Khurana D, Arneson LN, Schoon RA, Dick CJ, Leibson PJ. Differential regulation of human NK cell-mediated cytotoxicity by the tyrosine kinase Itk. J Immunol 2007;178:3575–82.
40. Gu H, You Q, Liu W, et al. Gambogic acid induced tumor cell apoptosis by T lymphocyte activation in H22 transplanted mice. Int Immunopharmacol 2008;8:1493–502.